SPECIAL
NOAA/EPA Golden Jubilee
ISSUE

Sand Flux Simulations at a Small Scale over a Heterogeneous Mesquite Area of the Northern Chihuahuan Desert

GEORGE E. BOWKER

Atmospheric Modeling Division, National Exposure Research Laboratory, U.S. Environmental Protection Agency, Research Triangle Park, North Carolina

DALE A. GILLETTE

Atmospheric Sciences Modeling Division, Air Resources Laboratory, National Oceanic and Atmospheric Administration, Research Triangle Park, North Carolina

GILLES BERGAMETTI AND BÉATRICE MARTICORENA

Laboratoire Interuniversitaire des Systèmes Atmosphériques, UMR CNRS 7583, Universités Paris 7-Paris 12, Créteil, France

DAVID K. HEIST

Atmospheric Sciences Modeling Division, Air Resources Laboratory, National Oceanic and Atmospheric Administration, Research Triangle Park, North Carolina

(Manuscript received 31 January 2006, in final form 23 May 2006)

ABSTRACT

Within areas of the Chihuahuan Desert dominated by honey mesquite bushes (*Prosopis glandulosa*), soil erosion causes open eroded patches and the formation of large coppice dunes. The airflow patterns around the dunes and through the open areas are correlated with sand flux and erosion. This study uses wind velocity simulations from the Quick Urban and Industrial Complex (QUIC) model in combination with a sand flux parameterization to simulate sand fluxes for each of eight storms occurring in the springs of 2003 and 2004. Total sand fluxes based on the sum of all the sand collectors located within the study domain were usually within 50% of the measured values for each of the storms, with simulations for individual sand collectors also often within 50% of the measured values. Simulated fluxes based on two different sand flux parameterizations were generally within 10% of each other, differing substantially only when the sand flux was low (near the threshold velocity). Good agreement between the field observations with a Sensit instrument and QUIC simulations for the same location and time series suggests that QUIC could be used to predict the spatial and temporal variation of sand flux patterns for a domain.

1. Introduction

In the northern part of the Chihuahuan Desert of New Mexico, the vegetation patterns have changed dramatically over the past 100 yr from a landscape dominated by black grama grass (*Bouteloua eriopoda*) to a dune landscape dominated by a mix of mesquite bushes (*Prosopis glandulosa*) and mesquite coppice dunes (Buffington and Herbel 1965). High-windstorms are common during the spring, often leading to wind erosion and redistribution of the soil around mesquite bushes and formation of coppice dunes that have grown to a height of up to 2 m in the time from 1900 to the present (Gibbens et al. 1983).

Understanding the airflow patterns and the resulting flux of sediment can enhance our understanding of desert sand movement and dust production. Furthermore, eolian sediment transport is important in redistributing plant nutrients, determining vegetation patterns, and contributing to the change in vegetation type (Schlesinger et al. 1990; Herbel et al. 1994). The Jornada Long-Term Ecological Research project

Corresponding author address: George Bowker, Atmospheric Modeling Division, National Exposure Research Laboratory, U.S. Environmental Protection Agency, Research Triangle Park, NC 27711.
E-mail: bowker.george@epa.gov

DOI: 10.1175/JAM2537.1

© 2007 American Meteorological Society

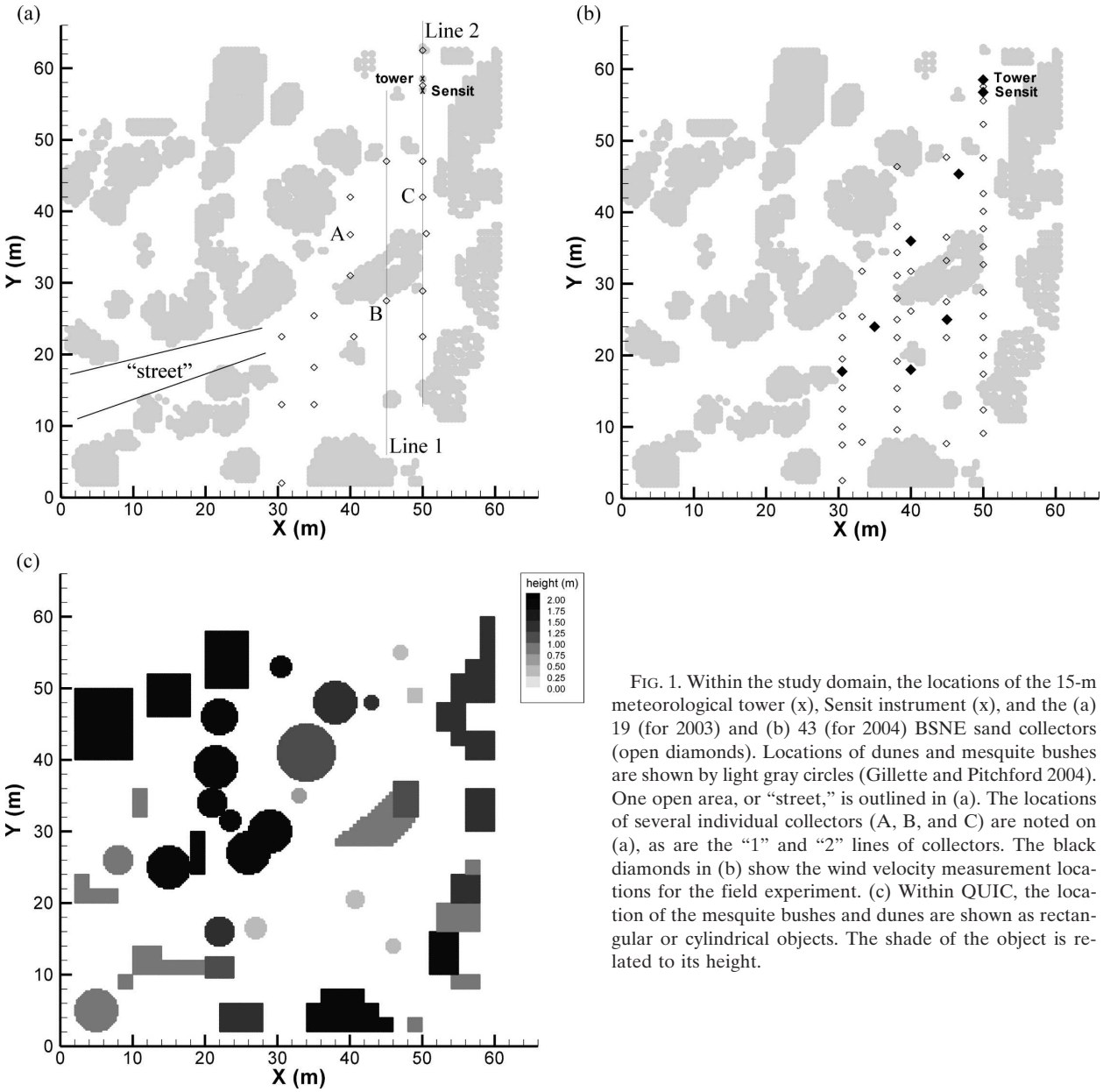

FIG. 1. Within the study domain, the locations of the 15-m meteorological tower (x), Sensit instrument (x), and the (a) 19 (for 2003) and (b) 43 (for 2004) BSNE sand collectors (open diamonds). Locations of dunes and mesquite bushes are shown by light gray circles (Gillette and Pitchford 2004). One open area, or "street," is outlined in (a). The locations of several individual collectors (A, B, and C) are noted on (a), as are the "1" and "2" lines of collectors. The black diamonds in (b) show the wind velocity measurement locations for the field experiment. (c) Within QUIC, the location of the mesquite bushes and dunes are shown as rectangular or cylindrical objects. The shade of the object is related to its height.

has since 1989 monitored net primary productivity (NPP) at several sites that are characteristic of the northern Chihuahuan Desert's principal ecosystems. We chose to monitor sand movement adjacent to the Jornada NPP sites to develop and evaluate models for studying eolian sediment production, transport, and deposition that are characteristic of the most important ecosystems of the northern Chihuahuan Desert. The specific site examined in this study, called Oriented by Gillette et al. (2006), is located in the Jornada Experimental Range, operated by the U.S. Department of Agriculture. Within the mesquite duneland area, there are large, elongated bare areas of sandy soil between mesquite bushes that are called streets by Okin and Gillette (2001). These streets are elongated in the same direction as the dominant wind at these sites: southwest to northeast (Gillette et al. 2004a) (Fig. 1a). These streets are exposed to strong winds, and thus wind erosion is a primary source of airborne sediments (Gillette and Pitchford 2004; Gillette et al. 2006). Gibbens et al. (1983) found, based on 45-yr-average changes in soil height, that open areas were decreasing by 0.0021 m yr^{-1} while the dunes were growing by 0.0024 m yr^{-1}.

Extensive field measurements of wind velocity were

made at this site during 2003 and 2004 (Gillette et al. 2006). Wind measurements (10-min time-average wind speeds) were made on a 15-m meteorological tower and on eight 3-m-high masts located within the 2-m-tall dunes (Fig. 1b). Each 3-m mast had three cup anemometers at approximately 0.75-, 1.5-, and 3-m heights. The wind measurements collectively give a rough picture of the wind patterns within and above the dunes at the site, providing insight into the sand flux patterns. During wind erosion episodes (high winds), measured Richardson numbers are close to zero, indicating near-neutral stability conditions (Gillette et al. 2006).

Bowker et al. (2006) simulated the wind field patterns for the site using the Quick Urban and Industrial Complex (QUIC) model, version 3.5, and compared the simulated winds with the field wind measurements. QUIC is a fast-processing mass-consistent, semiempirical wind field model developed by Los Alamos National Laboratory and the University of Utah (Pardyjak and Brown 2001, 2002; Williams et al. 2004). QUIC simulates the wind field patterns (ensemble-average solutions) for a complex domain by using empirically based solutions for the flow patterns around isolated rectangular or cylindrical obstacles and then applying mass consistency (continuity) to the resulting block assemblies. The empirically based solutions prescribe wake cavities, vortices, upwind recirculations, and areas of influenced flow around the blocks. The empirical aspects of the QUIC model are based on wind-tunnel and field studies that take place in near-neutral stability conditions. These conditions are similar to those of the field measurements (Gillette et al. 2006). Individual mesquite bushes and coppice dunes were incorporated into the model as assemblies of solid rectangular or cylindrical blocks. We chose to make the simplest model to see if some of the strongest features of the flow were reproduced. Such complexities as rounded mesquite bush shape and porosity were ignored. Figure 1 shows the basic geometry of the domain as measured in the field and as modeled in QUIC. The overall flow fields were described well, with QUIC correctly identifying areas of high flow and areas of wake flow (Fig. 2a). The 10-min-average wind velocities simulated by QUIC at 0.625 m are highly comparable to those measured in the field at 0.75 m and scaled to 0.625 m. They are often within several degrees of the direction and, on average, 6% less (25% standard deviation) in magnitude (Bowker et al. 2006). Figure 2b presents comparisons of wind speed for six locations at 0.625-m height for each of the 270 ten-minute time periods during the April 2003 and 2004 storms (Bowker et al. 2006). Some discrepancies were found, with QUIC underpredicting the wind speed for some locations and times. This may result from QUIC not showing as much change in wind direction associated with channeling of flow as observed in the field and sometimes overextending the size of the wake-flow regions (Bowker et al. 2006).

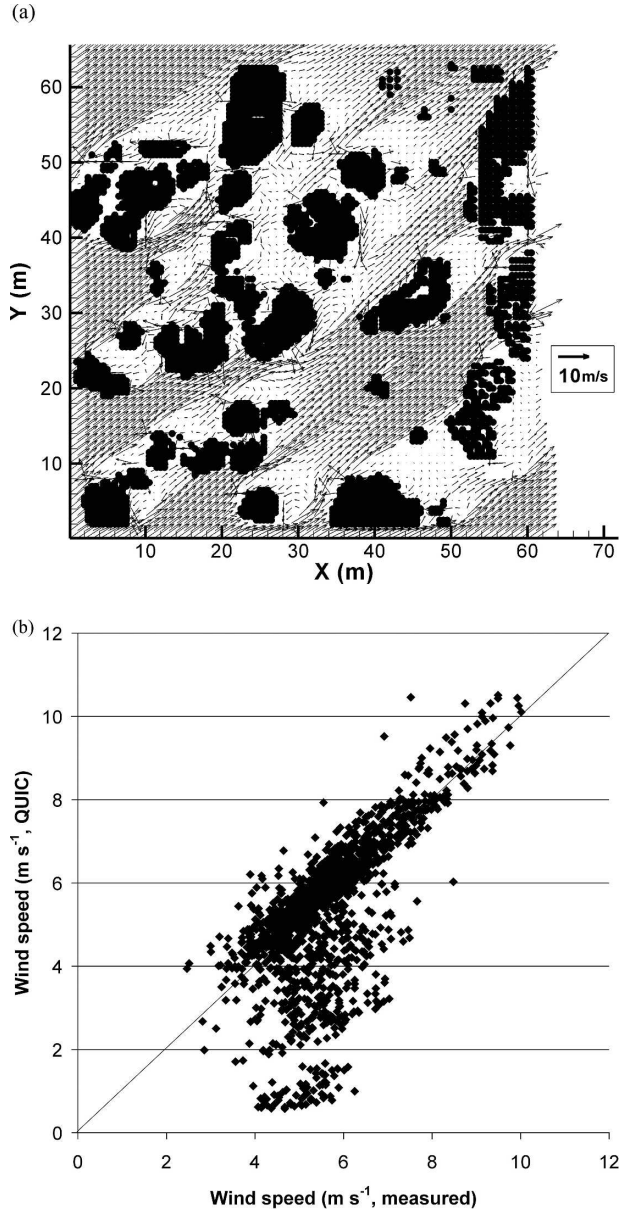

FIG. 2. (a) Wind velocity vectors (0.625-m height) at the study site (bushes and dunes are black) are shown for one 10-min time period on 15 Apr 2003. The reference wind velocity at 14.9 m was 15.3 m s^{-1} at 234°. (b) The comparison for six locations between all of the 10-min-averaged wind speeds measured in the field (scaled to a 0.625-m height) and the predictions made by QUIC.

The field measurements in combination with wind velocity simulations using the QUIC model have shown that the wind field patterns are highly complex and

heterogeneous within the area (Gillette et al. 2006; Bowker et al. 2006). Wind velocities are very large within the streets, ranging from 4 to 10 m s^{-1} at a height of 0.75 m. If the driving wind direction does not exactly align with the street, the dunes will steer the interdune wind by up to 20°, channeling it up the "streets." For high wind velocities (probably larger than 5 m s^{-1} at 0.75 m) and friction velocities (1.0 m s^{-1}, based on wind profiles from the 15-m tower), eolian erosion of the soil surface occurs within the streets. However, for every wind direction, both the field measurements and simulations suggest that there are open areas experiencing wake or interference flow. In these areas the wind velocity is low, less than about 4 m s^{-1} at 0.75 m, and the soil surface is likely not eroding. These areas are typically found on the lee of the coppice dunes. As the wind direction changes during a storm, the airflow patterns in the domain change. Locations experiencing wake flow for one wind direction may experience street flow for another. Sediment is eroded in high-wind areas exceeding the threshold friction velocity where sand first begins to move (around 0.25 m s^{-1}) (Gillette and Chen 2001; Marticorena et al. 1997). As a consequence, the sand flux patterns at the site are intimately tied to the airflow patterns.

In addition to the wind field measurements, monitoring of the sand flux for each sandstorm was performed in 2003 and 2004. As a preliminary step toward ultimately modeling erosion and deposition patterns for the entire domain, we decided to model sediment transport rates by linking the wind fields predicted by QUIC to an equation parameterizing sand flux as a function of wind velocity.

A number of equations have been proposed linking horizontal sand fluxes with wind velocities (Bagnold 1941; Zingg 1953; Williams 1964; Kawamura 1964; Owen 1964; Gillette and Goodwin 1974; Gillette 1979; Lettau and Lettau 1978; White 1979; Sörensen 1985; Gillette and Stockton 1989; Leys and Raupach 1991; Shao et al. 1993a; Stout and Zobeck 1997; Zheng et al. 2003, 2006; Stout 2004; Leenders et al. 2005). It is well established from these studies that sand flux is proportional to u_*^3 and, thus, to u^3, where u_* is the friction velocity and u is the wind speed. The sand flux equations have been developed for equilibrium conditions. We assume 1) that the sand supply is not limited, 2) that momentum flux to the surface from the wind can be expressed as the square of the friction velocity times the air density, and 3) that the situation is at equilibrium at each location. However, in some cases, we apply the equations in areas of complex roughness configurations that meet criteria 1 and 2 and not necessarily 3.

According to Shao (2000), small variations in one difficult-to-ascertain parameter found in many of the equation formulations (the wind threshold velocity, u_{*t}) contributes more uncertainty than the variability resulting from different equation formulations. He concluded that the equations proposed by Kawamura (1964), Owen (1964), Lettau and Lettau (1978), or White (1979) are all well adapted to simulate the horizontal sand flux.

The object of this study is to link the wind fields simulated by QUIC to a parameterized sand flux equation to model sand flux in space and time for the study site. We compare the sand flux model predictions with the field measurements and then assess the sensitivity of the simulations to several aspects such as the formulation of the sand flux equation and the specific value of the threshold velocity. If successful, this general approach, namely, applying a sand flux equation to the output of a high-resolution diagnostic wind field model, could be used to describe sand fluxes as well as erosion and deposition patterns for other desert locations.

2. Details of the wind and sediment flux data

a. Field measurements of sand flux

This study focuses on sand movement in the Oriented study site, characterized by large mesquite coppice dunes (up to 2 m in height) (Gillette et al. 2006). The study site is located at 332 370 m E and 3 610 380 m N in universal transverse Mercator coordinates (zone 13). During 2003 and 2004, sediment fluxes for eight individual sandstorms were collected using 19 and 46 Big Springs Number Eight (BSNE) collectors, respectively (Fryrear 1986). Collectors were added in 2004 to increase the resolution of the sand flux patterns. There were five sandstorms in April of 2003 and three smaller sandstorms in April of 2004. The locations of the BSNE catchers among the mesquite bushes at the site for 2003 and 2004 are shown in Figs. 1a,b, respectively. There were no drastic changes in the dune geometry and vegetation height between 2003 and 2004.

Details of these BSNE catchers and the integration of fluxes from the ground to 1-m height are given by Gillette and Chen (2001). These passive collectors maintained 90% efficiency for all winds (Shao et al. 1993b). They collected airborne particles at nominal heights of 0.05, 0.1, 0.2, 0.5, and 1 m above the surface. The measured horizontal mass flux for the five heights was fitted to an empirical formula used by Shao and Raupach (1992). After fitting measured sand flux accumulations $m(z)$ collected at height z to the Shao and Raupach (1992) equation, mass flux $Q = \int m(z)\, dz$ was integrated from 0 to 1 m above ground, because 90% or

more of the sand flux is found below 1 m for the wind speeds at this study site (Gillette et al. 2006).

In addition, a fast-response horizontal mass flux Sensit[1] instrument was placed within 1 m of the 15-m tower (Gillette and Stockton 1986; Stockton and Gillette 1990; Gillette et al. 2004a). The Sensit sensor was placed at a height of 0.05 m above the surface. The sensor consists of a ring of piezoelectric material mounted on a steel cylinder 0.025 m in diameter. It responds to particle impacts on the ring surface and converts the responses to counts. These sensors had been previously used by Stockton and Gillette (1990) to sense airborne sand movement. Calibration of the Sensit instrument showed that instrumental counts (in this case, to the 3/2 power) are roughly proportional to mass flux (Gillette et al. 1997b). A detailed calibration of a Sensit that was modified to respond to smaller kinetic energy but that was fundamentally similar to the Sensit instruments used in these field studies is given by Gillette et al. (2004b,c). These calibrations show that the Sensit has measurable thresholds for detection, has a point of saturation, and produces a signal that is roughly proportional to kinetic energy.

b. QUIC wind field simulations

Two-hundred-fifty-one QUIC simulations were made for the sandstorms observed in April of 2003. These times represented all 10-min periods during which sustained wind speeds measured at the 3-m masts were above 6.0 m s^{-1} (Gillette et al. 2006) and, based on Sensit activity, included virtually all times with measured sand flux. The simulations were made using an inlet boundary layer selected to match the field measurements of velocity at the lowest height available (0.75 m). The driving wind velocity for the simulations was the 10-min time-averaged wind velocity from the top of the 15-m tower (which is 6 times the tallest bush heights and, hence, is considered to be relatively uninfluenced by the local roughness elements) (Bowker et al. 2006). The study model setup was simulated within the QUIC model as a 66 m $\times$ 66 m $\times$ 5 m domain of cubical grid cells (0.25 m on a side). The 0.25-m grid spacing allowed adequate representation of the roughness elements while still maintaining a large area of study. The dimensions and locations of dunes and mesquite bushes are represented as shown in Fig. 1c. These are derived from field observations made by Gillette and Pitchford (2004). The wind velocity was output at 0.25-m increments starting at 0.125 m above the ground. The QUIC simulations were optimized for a height of 0.75 m by comparison between velocity measurements made in the field at 0.75 m and QUIC outputs from 0.625 and 0.875 m (Bowker et al. 2006). For this study, we will focus on results based on the velocity fields at 0.625 m (these velocity values were proportional to those from the 0.875-m height).

In addition, three more simulations were made for 2003 and 43 more simulations were made modeling the time period of April of 2004, spanning three sandstorms. These simulations were done using the same setup parameters described in detail by Bowker et al. (2006), including domain geometry, incoming boundary layer (characterized by a 0.017-m roughness length), and driving wind velocities (measured at 15 m). Additional parameters matched include the street-canyon vortex, upwind cavity, and "block top" flow algorithms.

3. Sand flux modeling

To test our ability to model sand flux using the simulated velocity fields, we compared the field measurements of total sand flux caught during a storm at each BSNE collector location with the cube of wind speed simulated at a height of 0.625 m also at each location for a single 10-min time period (Owen 1964; White 1979). The comparison was performed for a 10-min time period during a storm on 15 April 2003, corresponding to a period of high wind velocity and high sand flux (Fig. 2a). Even though this comparison is a rough estimate (because the event was much longer than 10 min in duration and the velocity patterns changed slightly every 10 min), Fig. 3 shows that for some locations the higher sand fluxes are measured where QUIC predicts the higher wind velocities. For the BSNE collectors along lines 1 and 2, where the velocities and sand fluxes were expected to be the highest, there is a possible correlation between the cube of wind speed and measured sand flux. This correlation suggests that it may be possible to predict sand fluxes based on QUIC wind fields and encourages us to attempt a more detailed comparison. Furthermore, this result also suggests that, for an area such as the study site, the main factor controlling where erosion occurs and how much sand is removed by wind is probably the wind velocity field. For some locations, the poor relationship between the cube of wind speed and cumulative (time integrated) measured sand flux suggests that this particular time increment may not be representative of the time periods of maximum sand flux.

[1] The names of commercial products do not imply an endorsement by the authors, the U.S. Department of Commerce, or the U.S. Environmental Protection Agency.

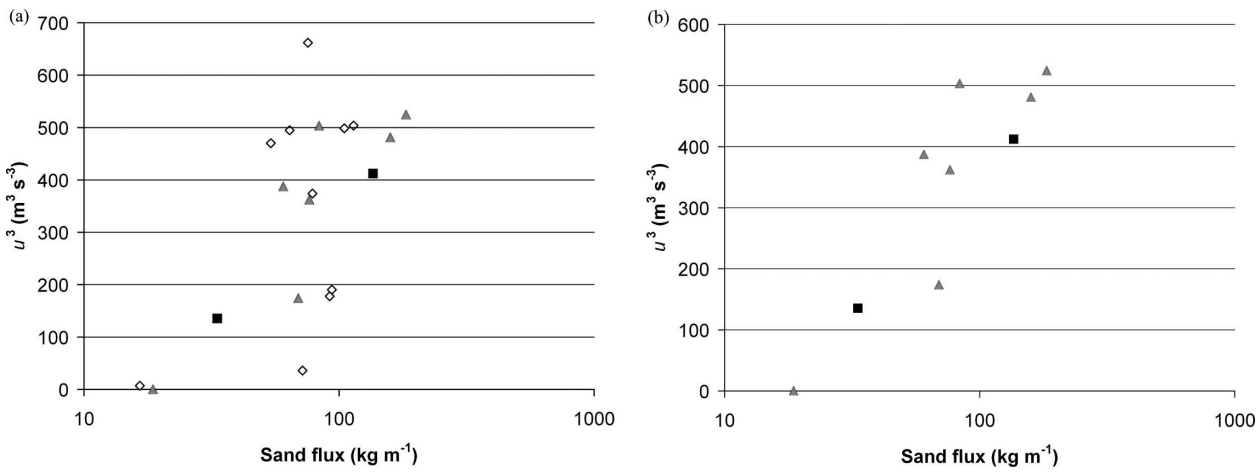

FIG. 3. Relationship between u^3 at each BSNE location as simulated by QUIC for a 10-min time period of high winds and BSNE sand flux measurements for the corresponding sandstorm (15 Apr 2003) (a) for all of the BSNE measurements (all symbols) and (b) only for BSNE on lines 1 (black squares) and 2 (gray triangles) (see Fig. 1a for the location of the lines).

a. Sand flux parameterizations

Using the wind velocities simulated by QUIC, it is possible to predict sand flux given a relationship between wind velocity and sand movement. We decided to test two sand flux parameterizations—one developed by Kawamura (1964) and used by White (1979) [Eq. (2)] and the other developed by Owen (1964) [Eq. (1)]. The two equations, which asymptotically converge at high wind speeds but have very different dependencies of the sand flux G on the erosion threshold, are

$$G = A_1 u_*^3 \left(1 - \frac{u_{*t}^2}{u_*^2} \right) \quad \text{and} \tag{1}$$

$$G = A_2 u_*^3 \left(1 - \frac{u_{*t}^2}{u_*^2} \right) \left(1 + \frac{u_{*t}}{u_*} \right), \tag{2}$$

where $A_1 = c_1\rho/g$ and $A_2 = c_2\rho/g$, ρ is the air density, g is gravitational acceleration, and c_1 and c_2 are constants, generally adjusted a posteriori on the measurements. By having both A_1 and A_2 be constant, we assume that the sediment availability does not vary between storms [i.e., there is no supply limitation; see Gillette and Chen (2001) for details on supply limitation for a nearby area] and that the threshold velocity does not depend on location. The two equations describe the flux through a tall, thin area perpendicular to the soil surface with dimensions 1 m wide by the height of the atmosphere. The parameterizations implicitly include the flux integration over the height of the atmosphere, and so the units are kilograms per meter per second, rather than kilograms per meter squared per second. To compare with the field data, we examine the flux over a 10-min time period for an area with a width of 0.01 m. Thus, the units of sand flux presented here will usually be in kilograms per meter per 10-min increment, or kilograms per meter per the duration of the storm.

Equations (1) and (2), while usually applied using the friction velocity and threshold friction velocity, can also be formulated by replacing u_* with u, a velocity at a particular height, and replacing u_{*t} with u_t, the threshold velocity derived from the velocity profile at the height. Because velocity at a particular height is a primary output of the QUIC model, the latter forms of Eqs. (1) and (2) are the most appropriate for these sand flux simulations.

The sand flux at each point within the domain at each 10-min time increment can be simulated using the velocity at 0.625 m at that point from QUIC and the appropriate threshold velocity for that height u_t. The total sand flux captured by a BSNE collector would equal the sum of the sand flux at its location for all the time increments during a storm.

b. Adjustment of these equations

Equations (1) and (2) can be applied using the wind speed simulated by the QUIC model. However, there are two "unknown" parameters (u_t and either A_1 or A_2). The constants were determined by fitting the total catch of all BSNE collectors for an individual storm with the total simulated time-integrated fluxes at the sediment collectors' locations to Eqs. (1) and (2).

A first approximation for u_t of 6.25 m s^{-1} was made based on the field time series of Sensit data and the

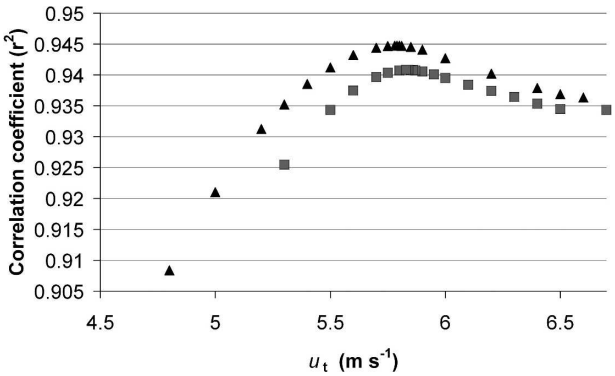

FIG. 4. Correlation coefficient r^2 as a function of applied threshold velocity (u_t; m s^{-1}) for the regression lines comparing the total sand fluxes from all BSNE locations for each of the eight sandstorms using the QUIC wind velocities at heights 0.625 m for the White (gray squares) and Owen (black triangles) equations and the field measurements. The optimal u_t value at 0.625 m is 5.8 m s^{-1}, for both Eqs. (1) and (2).

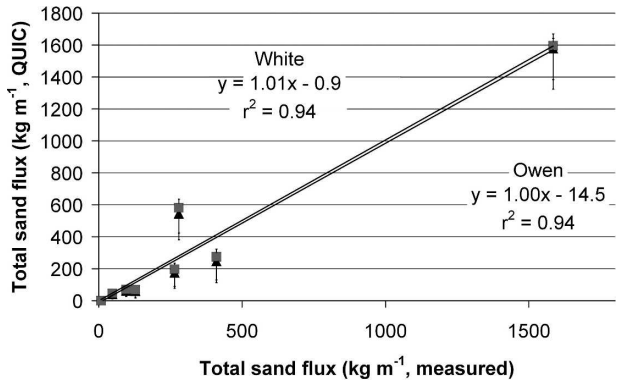

FIG. 5. A comparison between cumulative sand flux simulated (kg m^{-1}) for all BSNE locations as a function of flux measured (kg m^{-1}) for each of the eight storms occurring during 2003 and 2004. Solid black triangles and gray squares show the approximations based on the 0.625-m QUIC velocity predictions for the Owen and White equations, respectively, using the best-fit values (i.e., optimized constants u_t and A_1 or A_2). For each storm, the upper and lower error bars represent fluxes computed using values spanning the threshold velocity range (5.7 and 6.2 m s^{-1}) determined from the Sensit instrument measurements, but with the A_1 or A_2 constant remaining fixed.

wind speed at the lowest tower height of the 15-m tower (1.3 m). By scaling the threshold wind speed logarithmically (using a roughness length of 0.017 m), u_t at 0.75 m was estimated to be 5.5 m s^{-1}. Based on this value, A_1 and A_2 were estimated to be 0.000 017 and 0.000 008 kg s^2 m^{-4} for Eqs. (1) and (2), respectively. A refinement of the two constants was done as follows: using the starting values obtained as explained above, u_t was incrementally varied between 4.0 and 7.0 m s^{-1}. Based on the regression coefficient comparing the total simulated and measured sand accumulation for the eight storms, we obtained a "best fit" value for u_t of 5.8 m s^{-1} at 0.625 m for both Eqs. (1) and (2) (Fig. 4). Using the best-fit u_t, the values for the A_1 and A_2 constants needed to make the regression lines have a slope of unity were found to be 0.000 018 and 0.000 011 kg s^2 m^{-4} for the two equations, respectively (Fig. 5). The error bars for each storm (shown in Fig. 5, and described in section 3e) show the sensitivity of the resulting approximation to variation in the value of u_t, when the A_1 and A_2 constants are fixed at the best-fit values.

c. *Comparison with the wind velocity threshold derived from Sensit measurements*

To check the physical relevance of the threshold wind velocity determined by fitting the sand flux equations and measurements in section 3b, we compared the values with those derived from the Sensit measurements. The Sensit threshold wind velocity was determined based on the correlation between the Sensit counts and the wind velocity measured at the lowest level (0.75 m) for the closest mast (mast N) using the 2003 dataset (Fig. 6). The threshold velocity is the velocity at which sand first begins to move and should be where the Sensit first records nonzero readings, indicating that the mass flux of airborne sediment is no longer zero. At a height of 0.75 m, this transition appears to occur around 6.0 m s^{-1}. A roughly linear relationship exists between Sensit counts and the square of the wind velocity measured at 0.75 m (Table 1). The intercept provides the value of the square of the threshold wind velocity. Table 1 also shows the values of the threshold velocity at 0.75 m, which, when rescaled to 0.625 m for better comparison with the threshold determined by fitting, range between 5.7 and 6.2 m s^{-1} depending on the threshold we use for the Sensit counts (10-min time increments with just one, two, three, and four counts excluded from the fitting, in turn). The best-fit threshold velocity value (5.8 m s^{-1}) determined

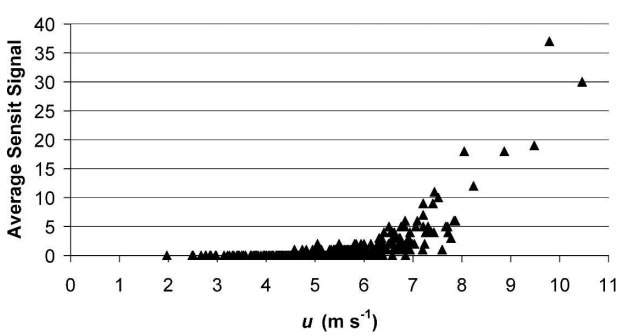

FIG. 6. The 10-min average of Sensit counts vs wind velocity measured at 0.75 m on mast N during the 2003 experiment.

TABLE 1. Threshold wind velocity derived from Sensit measurement for different thresholds of the number of Sensit counts. The statistical parameters of the regression between the Sensit counts and u^2 are given. An asterisk indicates a 99% significance level (p value of <0.01) for the confidence of the fit of the correlation.

Sensit threshold	No. of points	Slope	r^2	Intercept	u_t (0.75 m) (m s^{-1})	u_t (0.625 m) (m s^{-1})	F value
>0	158	2.21	0.66	35.83	5.99	5.70	301*
>1	70	1.93	0.75	39.69	6.30	6.00	209*
>2	44	1.81	0.78	41.75	6.46	6.15	151*
>3	35	1.77	0.79	42.39	6.51	6.20	122*
>4	24	1.79	0.81	41.98	6.48	6.17	91*

by fitting Eqs. (1) and (2) falls within the range of expected values.

d. *Sensitivity of the sand flux computation to the difference in parameterization*

To compare the sand flux parameterizations, we first predict the total sand fluxes captured by all of the BSNE for the eight sandstorms during 2003 and 2004 using each sand flux equation and the constants (u_t and either A_1 or A_2) obtained by fitting. Figure 5 shows that the two equations, when linked to the wind velocities simulated by QUIC, provide excellent agreement with the data: the correlation coefficients are very high (0.94) and (by definition) the slopes are very close to 1. QUIC is able to predict the total sand flux captured by the BSNE collectors for a storm, often to within 50% (Fig. 5).

When the relationship between the simulated sand fluxes and the measured flux for each individual BSNE for all of the sampled sandstorms is examined (Fig. 7), we observed that the two equations yield similar predictions. Both are able to predict the total sand flux at each BSNE location over the course of a storm, nearly always within an order of magnitude and often within 50%. As expected, both equations very precisely simulate the higher sand fluxes, whereas there are differences for the lowest sand fluxes. Some of the differences may result from inadequate simulation of the wind velocity patterns, or of the constants (u_t and the As) not being well matched for those locations or times. The relative differences between the two equations are usually low, less than 10% for all fluxes larger than 1.0 kg m^{-1} (Fig. 8). Moreover, the largest errors are observed for the lowest simulated fluxes, which are obviously of lesser interest for wind erosion assessment. In general, the White equation provides fluxes that are slightly larger than those computed using the Owen equation.

We can conclude that both equations adequately reproduce the measured sand fluxes accumulated over a storm at a given location and that for larger accumula-

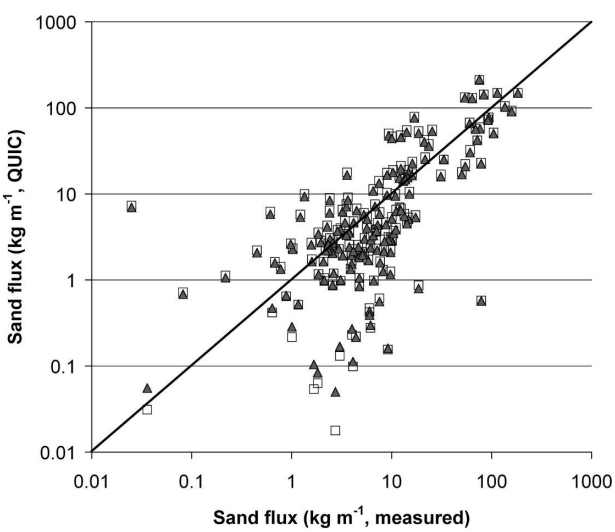

FIG. 7. Total sand flux (kg m^{-1}) predicted by QUIC for each storm for each BSNE collector as a function of the measured sand flux. Solid triangles and open squares show the approximations based on the 0.625-m velocity predictions for the Owen and White equations, respectively.

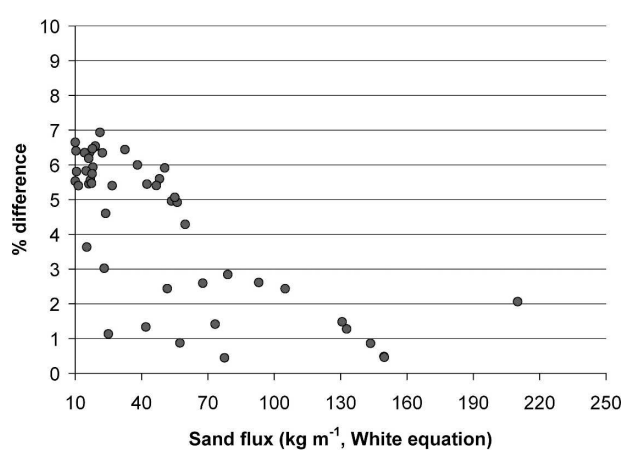

FIG. 8. The absolute value of the percent difference of the predicted sand flux (Owen − White)/White for each of the BSNE collectors for a single storm.

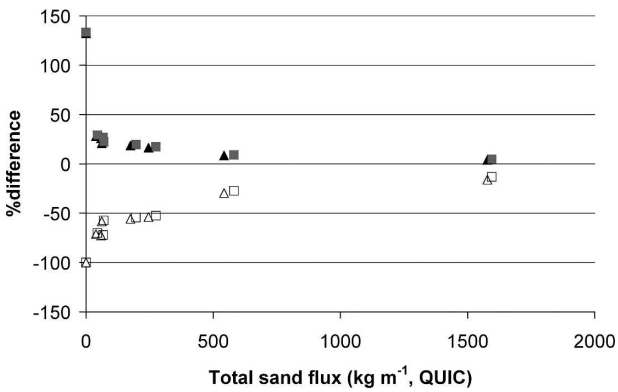

FIG. 9. For each of the eight storms, the percent difference between the best-fit flux and the fluxes computed using values spanning the threshold range determined from the Sensit (5.7 and 6.2 m s^{-1}), with constants (A_1 and A_2) remaining fixed, divided by the best-fit flux. The solid and open symbols refer, respectively, to the 5.7 and 6.2 m s^{-1} threshold velocities for both the Owen (triangles) and White equations (squares).

tions they agree within 10%, suggesting that either equation can be used with some confidence to simulate sand fluxes.

e. Sensitivity to the threshold wind velocity

The simulated horizontal sand fluxes are especially sensitive to variations in the threshold wind velocity (Shao 2000). This parameter is difficult to measure in the field and varies with environmental conditions, location, and time during the storm (Stout and Zobeck 1997). Thus, the variation in u_t extrapolated from the Sensit measurements is probably representative of the variation among storms and among some locations and, thus, presents us with an opportunity to see how environmental variation could influence the results. To evaluate how much this uncertainty affects our simulations, we performed two additional simulations using the extreme values for the threshold wind velocity determined by using the Sensit (i.e., 5.7 and 6.2 m s^{-1}) to bracket the range of the threshold value. Figure 5 shows how the total sand catch for each of the eight storms changes as the threshold value is changed in the sand flux equation. Increasing the threshold velocity dramatically decreases sand fluxes, suggesting that many of the sand collectors are experiencing velocities near threshold for many occasions.

In general, the agreement between simulated and measured sand fluxes for each storm remains reasonably good. The relative errors generated by changing the threshold wind velocities are on the order of 75% for the low measured sand fluxes (i.e., during periods for which the wind speed is close to the threshold and the sand flux is low) (Fig. 9, or Table 2). It is obvious that, for these situations in which the wind speed is relatively low, a small change in the value of the threshold friction velocity can generate very large errors. However, because the wind speeds (and, thus, the sand fluxes) are small, these errors do not dramatically influence the sand movement budget for the area. More significant are the errors for the higher sandstorms, which are of larger interest for the evaluation of the soil erosion by wind. For such events, the errors remain low, ranging between −16% and 5% (Fig. 9, or Table 2).

Thus, we conclude that variations in the threshold velocity affect our capability to simulate sandstorms of low intensity correctly but do not dramatically affect our simulations of the strong sandstorms.

f. Time- and space-resolved sand fluxes for each sand catcher

As shown in Fig. 7, the QUIC wind velocities, when linked to a sand flux equation, often predict the total flux captured by a single BSNE through the course of a single storm to within 50%. As expected, the predictions are reasonable for powerful storms, because the wind velocities are all well above threshold and the differences between the Owen and White equations are small. The largest relative differences between pre-

TABLE 2. Total accumulated sand flux for each of the eight storms. The percent over- or underpredictions are based on the best-fit Owen or White predictions.

	Measured (kg m^{-1})	Best fit (Owen) (kg m^{-1})	Best fit (White) (kg m^{-1})	Owen u_t = 5.7 m s^{-1} (%)	Owen u_t = 6.2 m s^{-1} (%)	White u_t = 5.7 m s^{-1} (%)	White u_t = 6.2 m s^{-1} (%)
Storm 1, 2003	410.3	245.5	274.7	16.4	−53.9	17.3	−52.6
Storm 2, 2003	95.3	61.8	69.5	21.0	−58.3	22.1	−57.3
Storm 3, 2003	1584.4	1577.9	1595.0	4.0	−16.1	4.7	−13.3
Storm 4, 2003	47.7	39.2	44.8	28.1	−71.1	29.1	−70.2
Storm 5, 2003	279.3	542.8	581.8	8.4	−29.7	9.2	−27.3
Storm 1, 2004	8.0	0.1	0.1	132.2	−100.0	133.1	−100.0
Storm 2, 2004	127.8	59.4	67.6	25.9	−72.6	26.9	−72.2
Storm 3, 2004	264.6	174.7	196.2	18.6	−55.7	19.5	−54.4

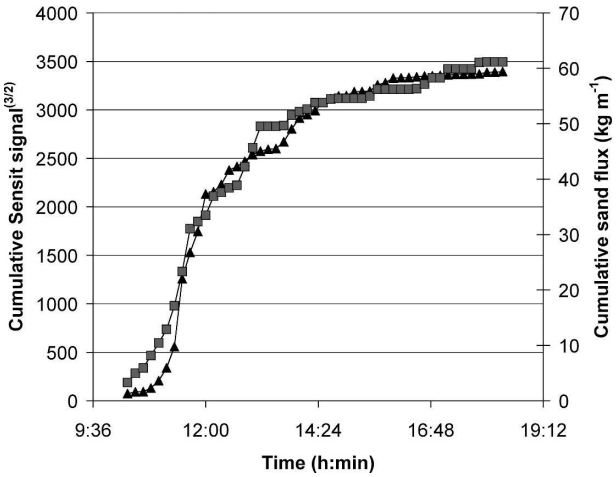

FIG. 10. Cumulative Sensit counts to the 3/2 power (solid triangles) as a function of time, plotted with predicted cumulative sand flux (kg m^{-1}) from the White equation (solid squares) at the Sensit location for the largest storm on 15 Apr 2003.

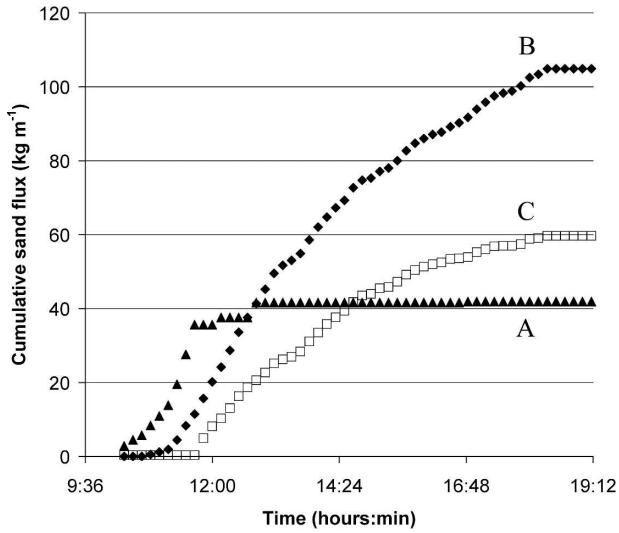

FIG. 11. Accumulated sediment as a function of time for three BSNE sand collectors (A, B, and C; see Fig. 1a for locations), based on the 10-min simulated sand fluxes (using the White equation) for the storm on 15 Apr 2003. The cumulative sand flux measured for each of these sand collectors (A, B, and C) in the field was 71.9 kg m^{-1}, 135.9 kg cm^{-1}, and 76.5 kg m^{-1} for this storm.

dicted and measured sand fluxes were found for the BSNE with the lowest flux capture. It is likely that these fluxes are very sensitive to small variations in conditions at the microscale. Thus, small inaccuracies in the model (e.g., local geometry, threshold friction velocity, or airflow patterns) could lead to these differences. The wind patterns and wind speeds vary throughout each storm, generally shifting from weak southerly winds to stronger southwesterly or westerly winds. As the wind direction shifts, locations can change between strong "street" flow and wake-flow conditions. Very few locations experienced continual street flow, regardless of the wind direction variations.

Because the sand flux patterns depend on the wind velocity patterns, which vary markedly throughout the domain and change with wind direction, it is likely that variation is also present in the time-resolved sand flux capture by the BSNE collectors. However, the BSNE collectors do not show time-resolved capture, but only show the total accumulation for an entire storm. The Sensit is the only instrument at the field site with time-resolved sand flux measurements. Thus, to show that the flux predicted by QUIC for any particular 10-min time increment is related to the sand flux in the field, we compared the time-resolved cumulative Sensit counts and cumulative predicted sand flux using the White equation at the Sensit's location for the course of a single storm (storm 3, in 2003) (Fig. 10). Considering that the Sensit signal is roughly proportional to the square of velocity (Table 1) and sand flux is proportional to the cube of velocity [Eqs. (1) and (2)], Sensit counts to the 3/2 power are roughly proportional to sand flux. Sensit counts to the 3/2 power are represented hereinafter as "Sensit counts$^{(3/2)}$." The sand flux based on velocities from QUIC linked to a sand flux parameterization can be used to successfully predict the Sensit count$^{(3/2)}$ patterns for each time increment.

It is consequently possible to calculate the sand flux patterns for each location within our mesquite domain for each 10-min time increment. The cumulative sand flux at three locations coinciding with three different BSNE collectors for the storm on 15 April 2003 are shown in Fig. 11. The sand flux patterns are clearly different, with one collector capturing a large quantity of sand during the first few minutes of the storm and others having much more gradual and continual capture.

g. *Uncertainty of QUIC model results*

The one source of error not described well in this paper is the error resulting from inaccuracies in the calculated wind field (either with empirical formulation of the model flows, or derived from problems with geometry, representation of mesquite by solid blocks, or the input boundary layer). Although wind velocities predicted for the study site often correlated well with field measurements, for some locations such as wake-flow regions and regions in fast channeling flow, QUIC underpredicted velocities (Bowker et al. 2006). This certainly accounts for some of the discrepancy between the sand flux measurements and predictions. However, specification of the threshold velocity also accounts for

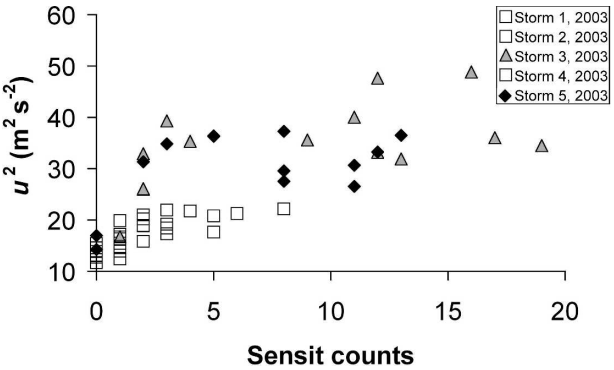

FIG. 12. The square of the wind speed predicted by QUIC at the Sensit location as a function of measured Sensit counts (for the wind direction measured at the 15-m tower between 220° and 239°).

some of the variation. In the field, the threshold velocity will certainly vary with time and location (and perhaps even wind direction).

A difference between measurement and simulation was notable for storm 5 in 2003. The sand fluxes at many BSNE locations for this storm were substantially overestimated (by a factor of approximately 2) by both equations. Including this storm changed the best-fit constants (u_t and A_1 or A_2) for the sand flux equations, raising the former and lowering the latter (Fig. 7). As a consequence, sand fluxes for many of the other storms were substantially underestimated. Storm 5 in 2003 was a strong storm but occurred shortly after the largest storm of the season (storm 3). Thus, we suspect that much of the available sediment had already been moved by storm 3 and that storm 5 was "supply limited" (Gillette and Chen 2001). Figure 12 shows that similar Sensit counts were obtained for storm 5 as for much weaker storms, indicating that not as much sediment was blowing in the wind, despite strong winds. However, the predominant wind direction for storm 5 (around 240°) was more westerly than for other storms, and so it is possible that the wind velocity simulations are overestimating wind speeds throughout the domain for these wind directions.

Other factors influencing sand flux, not included in the sand flux parameterizations used here and not captured within the QUIC wind field simulations, could improve the predictions. Based on measurements at the "scrape" site, Gillette and Chen (2001) identified several effects that influence sand flux. Located a few kilometers from and sharing similar soil characteristics, topography, and upwind vegetation with the study site, the scrape site is a flat, open area devoid of vegetation (Gillette and Chen 2001). At the scrape site, the flux of sand increased with distance downwind of the boundary where the mesquite vegetation stopped and the flat, bare surface began. This increase of sand flux is likely to be caused by aerodynamic effects (the Owen effect), particle–particle interactions, reattachment of boundary layers, and changes in the soil in the path of the wind erosion (Gillette et al. 1996, 1997a,b). Inclusion of these effects in the sand flux parameterization could lead to improved sand flux predictions.

4. Summary

Understanding sand flux patterns in highly complex terrain provides insight into desertification and the production of highly transportable dust. By linking the wind velocity patterns simulated by the QUIC model to a sand flux parameterization, we were able to simulate and reproduce field measurements of sand flux for a heterogeneous study site in the northern Chihuahuan Desert in New Mexico. This opens the possibility for creating high-resolution patterns of sand flux as well as extrapolating locations of sediment erosion and deposition for the entire study domain. Sand flux patterns could be analyzed for a larger region by dividing it into a number of smaller areas, each of which could be modeled using the technique developed here. These areas could then collectively be used to create parameterizations for an even larger scale of land that may have less detailed surface and vegetative characterization. For a small sensitive area with known terrain and vegetation, it may be possible to predict times of erosion and locations within the area that are particularly sensitive to erosion.

For this study, using values for the constants (u_t and A_1 or A_2) that were optimized based on the sand flux field data and found to be consistent with onsite Sensit measurements, we were able to simulate (within about 50%) sand flux measurements at each of the BSNE collector locations. The sand flux predictions depend on several factors, including the quality of the wind fields simulated by QUIC, the particular formulation of the sand flux parameterization, and the values of the constants used within the parameterization. Simulated sand fluxes based on the two sand flux Eqs. (1) and (2) were similar, differing by less than 10% for nearly all cases. For the third storm of 2003 (a high-flux situation), both simulations differed, on average, by less than 60% from each of the on-site measurements. The high-flux situations are the most important for describing sand movement in the domain and for practical assessment of windstorm damage.

Some of the difference between sand flux predictions and measurements may be attributable to the possibility that the parameters within the sand flux equations

(u_t and A_1 or A_2) are not constant, but vary slightly with location and with time (between storms) as supply limitation and soil aggregate structure change (Gillette and Chen 2001). Increasing the threshold velocity in the simulations decreased sand flux predictions, implying that velocities at 0.625 m at many BSNE collectors are near the threshold velocity for many time periods during the storm. Thus, the simulation is somewhat sensitive to our choice of parameters (u_t and A_1 or A_2). However, we expect that the differences between measured and simulated capture can mostly be attributed to differences in the actual wind field patterns and what is simulated within QUIC. Bowker et al. (2006) found differences between simulated and measured wind velocities for this domain, with QUIC sometimes underestimating wind velocities in wake zones and not describing as much acceleration of flow within the streets. The discrepancies could be due to differences in geometry, differing input boundary layer parameters, and modeling porous rounded bushes/dunes with the solid rectangular blocks.

However, for the small area in the northern Chihuahuan Desert, we conclude that when QUIC wind field simulations are linked to a sand flux parameterization, we are able to predict (within about 50%) total sand flux capture for all BSNE collectors for an entire sandstorm. In general, the flux patterns were predicted, with simulated and measured integrated flux collection for many individual BSNE collectors often within 50%. We found a good correlation between the real-time Sensit measurement and the sand flux predicted at the Sensit's location for each 10-min time increment. This suggests that the flux patterns for the domain for each time increment may be characteristic of the patterns present in the field.

Acknowledgments. Mr. Ashok Patel carefully carried out model runs. We also thank Steve Perry for insightful discussions about the subject. The research presented here was performed under the memorandum of understanding between the U.S. Environmental Protection Agency (EPA) and the U.S. Department of Commerce's National Oceanic and Atmospheric Administration (NOAA) under Agreement Number DW13921548. Although it has been reviewed by the EPA and NOAA and approved for publication, it does not necessarily reflect their policies or views. The U.S. government's right to retain a nonexclusive royalty-free license in and to any copyright is acknowledged.

REFERENCES

Bagnold, R. A., 1941: *The Physics of Blown Sand and Desert Dunes*. Chapman and Hall, 265 pp.

Bowker, G. E., D. A. Gillette, G. Bergametti, and B. Marticorena, 2006: Modeling flow patterns in a small vegetated area in the northern Chihuahuan Desert using QUIC (Quick Urban & Industrial Complex). *Environ. Fluid Mech.,* **6,** 359–384.

Buffington, L. C., and C. H. Herbel, 1965: Vegetational changes on a semidesert grassland range from 1858 to 1963. *Ecol. Monogr.,* **35,** 139–164.

Fryrear, D. W., 1986: A field dust sampler. *J. Soil Water Conserv.,* **41,** 117–120.

Gibbens, R., J. Tromble, J. Hennessy, and M. Cardenas, 1983: Soil movement in mesquite dunelands and former grasslands of Southern New Mexico from 1933 to 1980. *J. Range Manage.,* **36,** 145–148.

Gillette, D. A., 1979: Environmental factors affecting dust emission by wind erosion. *Saharan Dust, SCOPE 14,* C. Morales, Ed., John Wiley and Sons, 71–91.

——, and P. A. Goodwin, 1974: Microscale transport of sand-sized soil aggregates eroded by wind. *J. Geophys. Res.,* **79,** 4080–4084.

——, and P. H. Stockton, 1986: Mass, momentum and kinetic energy fluxes of saltating particles. *Aeolian Geomorphology,* W. G. Nickling, Ed., Allen and Unwin, 35–56.

——, and ——, 1989: The effect of nonerodible particles on wind erosion of erodible surfaces. *J. Geophys. Res.,* **94,** 12 885–12 893.

——, and W. Chen, 2001: Particle production and aeolian transport from a "supply-limited" source area in the Chihuahuan desert, New Mexico, United States. *J. Geophys. Res.,* **106,** 5267–5278.

——, and A. Pitchford, 2004: Sand flux in the northern Chihuahuan desert, New Mexico, USA, and the influence of mesquite-dominated landscapes. *J. Geophys. Res.,* **109,** F04003, doi:10.1029/2003JF000031.

——, G. Herbert, P. Stockton, and P. Owen, 1996: Causes of the fetch effect in wind erosion. *Earth Surf. Processes Landforms,* **21,** 641–659.

——, D. W. Fryrear, J. B. Xiao, P. Stockton, D. Ono, P. J. Helm, T. E. Gill, and T. Ley, 1997a: Large-scale variability of wind erosion mass flux rates at Owens Lake, 1, Vertical profiles of horizontal mass fluxes of wind-eroded particles with diameter greater than 50 μm. *J. Geophys. Res.,* **102,** 25 977–25 988.

——, E. Hardebeck, and J. Parker, 1997b: Large-scale variability of wind erosion mass flux rates at Owens Lake, 2, Role of roughness change, particle limitation, change of threshold friction velocity, and the Owen effect. *J. Geophys. Res.,* **102,** 25 989–25 998.

——, D. Ono, and K. Richmond, 2004a: A combined modeling and measurement technique for estimating windblown dust emissions at Owens (dry) Lake, California. *J. Geophys. Res.,* **109,** F01003, doi:10.1029/2003JF000025.

——, R. E. Lawson Jr., and R. S. Thompson, 2004b: A "test of concept" comparison of aerodynamic and mechanical resuspension mechanisms for particles deposited on field rye grass (*Secale cercele*), Part 1. Relative particle flux rates. *Atmos. Environ.,* **38,** 4789–4797.

——, ——, and ——, 2004c: A "test of concept" comparison of aerodynamic and mechanical resuspension mechanisms for particles deposited on field rye grass (*Secale cercele*), Part 2. Threshold mechanical energies for resuspension particle fluxes. *Atmos. Environ.,* **38,** 4799–4803.

——, J. Herrick, and G. Herbert, 2006: Wind characteristics of mesquite streets in the northern Chihuahuan Desert, New Mexico, USA. *Environ. Fluid Mech.,* **6,** 241–275.

Herbel, C. H., L. H. Gile, E. L. Fredrickson, and R. P. Gibbens, 1994: Soil water and soils at soil water sites, Jornada Experimental Range. *Supplement to the Desert Project Soil Monograph: Soils and Landscapes of a Desert Region Astride the Rio Grande Valley near Las Cruces, New Mexico,* Vol. 1, L. H. Gile and R. J. Ahrens, Eds., Soil Survey Investigations Report 44, U.S. Department of Agriculture, 592 pp.

Kawamura, R., 1964: Study of sand movement by wind. University of California Hydraulics Engineering Laboratory Rep. HEL 2-8. First published in Institute of Science and Technology, Report 5, 95–112, 1951.

Leenders, J. K., J. H. van Boxel, and G. Sterk, 2005: Wind forces and related saltation transport. *Geomorphology,* **71,** 357–372.

Lettau, K., and H. Lettau, 1978: Experimental and micrometeorological field studies of dune migration. Exploring the World's Driest Climate, K. Lettau and H. Lettau, Eds., University of Wisconsin—Madison IES Rep. 101, 110–147.

Leys, J. F., and M. R. Raupach, 1991: Soil flux measurements using a portable wind erosion tunnel. *Aust. J. Soil Res.,* **29,** 533–552.

Marticorena, B., G. Bergametti, D. A. Gillette, and J. Belnap, 1997: Factors controlling threshold friction velocity in semiarid and arid areas of the United States. *J. Geophys. Res.,* **102,** 23 277–23 287.

Okin, G. S., and D. A. Gillette, 2001: Distribution of vegetation in wind-dominated landscapes: Implications for wind erosion modeling and landscape processes. *J. Geophys. Res.,* **106,** 9673–9683.

Owen, P. R., 1964: Saltation of uniform grains in air. *J. Fluid Mech.,* **20,** 225–242.

Pardyjak, E. R., and M. J. Brown, 2001: Evaluation of a fast-response urban wind model: Comparison to single building wind-tunnel data. *Proc. Third Int. Symp. on Environmental Hydraulics,* Tempe, AZ, International Association of Hydraulic Engineering and Research, 6 pp. [Available from Los Alamos National Laboratory as LA-UR-01-4028.]

——and ——, 2002: Fast response modeling of a two building urban street canyon. *Proc. Fourth Symp. Urban Environment,* Norfolk, VA, Amer. Meteor. Soc., CD-ROM, J1.4.

Schlesinger, W. H., J. F. Reynolds, G. L. Cunningham, L. F. Huenneke, W. M. Jarrell, R. A. Virginia, and W. G. Whitford, 1990: Biological feedbacks in global desertification. *Science,* **247,** 1043–1048.

Shao, Y., 2000: *Physics and Modelling of Wind Erosion*. Kluwer Academic, 393 pp.

——, and M. R. Raupach, 1992: The overshoot and equilibration of saltation. *J. Geophys. Res.,* **97,** 20 559–20 564.

——, ——, and P. A. Findlater, 1993a: Effect of saltation bombardment on the entrainment of dust by wind. *J. Geophys. Res.,* **98,** 12 719–12 726.

——, G. H. McTainsh, and J. F. Leys, 1993b: Efficiency of sediment samplers for wind erosion measurement. *Aust. J. Soil Res.,* **31,** 519–531.

Sörensen, M., 1985: Estimation of some Aeolian saltation transport parameters from transport rate profiles. *Proc. Int. Workshop on the Physics of Blown Sand,* Vol. 1, Aarhus, Denmark, University of Aarhus, 141–190.

Stockton, P., and D. A. Gillette, 1990: Field measurements of the sheltering effect of vegetation on erodible land surfaces. *Land Degrad. Rehabil.,* **2,** 77–85.

Stout, J. E., 2004: A method for establishing the critical threshold for aeolian transport in the field. *Earth Surf. Processes Landforms,* **29,** 1195–1207.

——, and T. M. Zobeck, 1997: Intermittent saltation. *Sedimentology,* **44,** 959–970.

White, B. R., 1979: Soil transport by wind on Mars. *J. Geophys. Res.,* **84,** 4643–4651.

Williams, G., 1964: Some aspects of the eolian saltation load. *Sedimentology,* **3,** 257–287.

Williams, M., M. Brown, D. Boswell, B. Singh, and E. Pardyjak, 2004: Testing of the QUIC-PLUME model with wind-tunnel measurements for a high-rise building. *Proc. Fifth Conf. on Urban Environment,* Vancouver, BC, Canada, Amer. Meteor. Soc., CD-ROM, J5.3.

Zheng, X. J., N. Huang, and Y.-H. Zhou, 2003: Laboratory measurement of electrification of wind-blown sands and simulation of its effect on sand saltation movement. *J. Geophys. Res.,* **108,** 4322, doi:10.1029/2002JD002572.

——, ——, and Y. Zhou, 2006: The effect of electrostatic force on the evolution of sand saltation cloud. *Eur. Phys. J. E,* **19,** 129–138.

Zingg, A. W., 1953: Wind tunnel studies of the movement of sedimentary material. *Proc. Fifth Hydraulics Conf.,* Bulletin 34, Iowa City, IA, Institute of Hydraulics, 111–135.